

Limitations of the whole cell patch clamp technique in the control of intracellular concentrations

Richard T. Mathias, Ira S. Cohen, and Carlos Oliva

Department of Physiology and Biophysics, State University of New York at Stony Brook, Stony Brook, New York 11794 USA

ABSTRACT Recent experimental studies (Pusch and Neher, 1988) and theoretical studies (Oliva et al., 1988) have found that the pipette tip is a significant barrier to diffusion in the whole cell patch clamp configuration. In this paper, we extend the theoretical analysis of fluxes between the pipette and cell to include transmembrane fluxes. The general conclusions are: (a) within the pipette, ion fluxes are driven primarily by diffusion rather than voltage gradients. (b) At steady state there is a concentration difference between the bulk pipette and intracellular solution that is described by $\Delta c = jR_p/D\rho$, where $\Delta c = 1$ mM for a flux, $j = 1$ fmol/s, through a pipette of resistance, $R_p = 1$ M Ω , filled with a solution of resistivity, $\rho = 100$ Ω —cm, given a solute diffusion coefficient, $D = 10^{-5}$ cm²/s. (c) The time to steady state is always accelerated by membrane transport, regardless of the direction of transport.

We apply our analysis to the measurement of transport by the Na/K pump and Na/Ca exchanger in cells from the ventricles of mammalian heart. We find that the binding curve for intracellular Na⁺ to the Na/K pump will appear significantly less steep and more linear if one does not correct for the concentration difference between intracellular and pipette Na⁺. Similar shifts in the binding curve for extracellular Na⁺ to the Na/Ca exchanger can occur due to depletion of intracellular Ca⁺⁺ when the exchanger is stimulated. Lastly, in Appendix we analyze the effects of mobile and fixed intracellular buffers on the movement of Ca⁺⁺ between the pipette and cell. Fixed buffers greatly slow the time for equilibration of pipette and intracellular Ca⁺⁺. Mobile buffers act like a shuttle system, as they carry Ca⁺⁺ from pipette to cell then diffuse back when they are empty. Vigorous transport by the Na/Ca exchanger depletes mobile buffered calcium, thus stimulating diffusion from the pipette to match the rate of Ca⁺⁺ transport. Moreover, we find that binding of Ca⁺⁺ to the exchanger can be affected by the mobile buffer.

INTRODUCTION

The whole cell patch clamp technique offers the opportunity to modify transmembrane voltage and the ionic environment on both sides of the cell membrane. This represents a significant advance in our ability to characterize quantitatively the dependence of membrane ion pumps and exchangers on those parameters which affect them most directly. The degree to which we modify the voltage or ionic concentrations, however, must be carefully characterized if the quantitative information is to be most useful.

In a recent report (Oliva et al., 1988), we analyzed the time for a solute in the patch pipette to equilibrate with the intracellular space. Although this analysis considered impermeant solutes that were not buffered intracellularly, one important and general prediction was that the pipette tip represented the dominant barrier to diffusion. As a consequence, we were able to describe the time course of equilibration with a single exponential whose time constant depended entirely on experimentally accessible parameters. At about the same time, Pusch and Neher (1988) published an elegant experimental study of exactly the situation which we were modeling. They ob-

served that the time course of equilibration was a single exponential whose time constant depended qualitatively on the experimental parameters which were predicted by our model. Moreover, we found that our model predicted quantitatively their observed time constants, given all of the experimental parameters that they reported, and given that the solute was impermeant. From this close agreement of experiment with theory, we conclude that the pipette tip is indeed the rate limiting barrier to diffusion.

The existence of a large barrier to the cell interior through the pipette tip raises an additional important question concerning the study of membrane transport properties. If the cell membrane area is large and the cell transport rate is elevated, can the pipette supply sufficient quantities of a transported substance? In other words, is the pipette concentration a reasonably accurate estimate of the concentration of the transported substance within the cell? Accurate studies of membrane transport require knowledge of the cell's ionic concentrations, but elevated transport rates require significant fluxes across the pipette tip and, consequently, significant gradients of the trans-

ported substance between the bulk pipette solution and the cell interior. It is this situation which the present study was designed to investigate.

GLOSSARY

a	Distance of perfusion from pipette tip (cm)
A	Cross-sectional area of the pipette shank (cm ²)
c	Total concentration, both free and bound to mobile buffers, of an arbitrary solute within the cell and pipette (mol/cm ³)
c_e	Total concentration of an arbitrary extracellular solute (mol/cm ³)
c_i	Average value of c within the cell (mol/cm ³)
c_o	Some fixed value of intracellular concentration (c_i) (mol/cm ³)
c_p	Value of c in the bulk pipette solution (mol/cm ³)
C_i	Normalized intracellular concentration (Eq. 16)
C_p	Normalized pipette concentration (Eq. 16)
D	Diffusion coefficient for solute c (cm ² /s)
i_h	Holding current applied to voltage clamp the cell (A)
J_T	Maximum transmembrane transport of an intracellular solute out of the cell with all binding sites saturated (mol/s)
j_T	Transmembrane transport of solute c_i (mol/s)
j_L	Transmembrane passive leak of c_i (mol/s)
j	Net transmembrane flux out of the cell $j = j_T + j_L$ (mol/s)
j_o	Net flux of c_i across the membrane at $c_i = c_o$ (mol/s)
K_e	Binding constant for c_e to the transport protein (mol/cm ³)
K_i	Binding constant for c_i to the transport protein (mol/cm ³)
$P_i^n(c_i)$	Probability of c_i binding to n independent intracellular sites on the transport protein
$P_e^m(c_e)$	Probability of c_e binding to m independent extracellular sites on the transport protein
R_p	Resistance of the pipette shank (Ω)
S_m	Surface membrane area of the cell (cm ²)
T	Time of peak flux (s)
V_i	Intracellular volume (cm ³)
ρ	Resistivity of the pipette filling solution (Ω cm)
τ_T	Time constant for transport from the cell (Eq. 15) (s)
τ_p	Time constant of diffusion from the pipette (Eq. 10) (s)
τ_b	Time constant to change the extracellular bath (s)
ψ	Voltage at an arbitrary location in the pipette or cell (V)

THEORY

Fig. 1 illustrates the geometry and some of the assumptions associated with our analysis. A patch is formed and sucked out making an interface between the pipette solution and intracellular solution at $x = 0$. The concen-

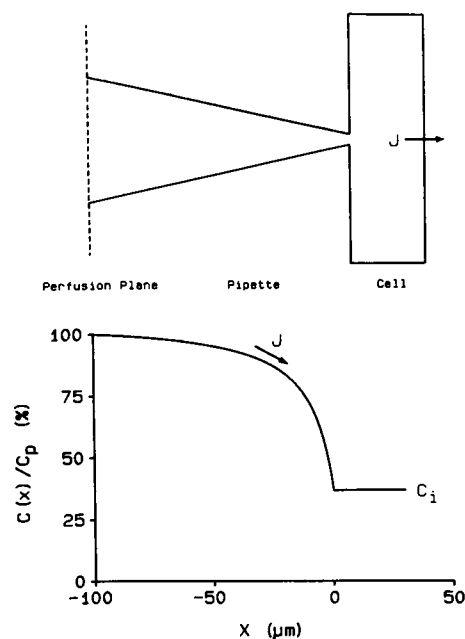


FIGURE 1 The upper panel represents a pipette attached in the whole cell patch clamp configuration to a cell of arbitrary shape. The cell is assumed to transport a solute of intracellular concentration c_i at a net rate j . The lower panel illustrates the expected steady state concentration profile. The pipette is assumed to be perfused at a distance of 100 μ m from the patch, hence, the pipette concentration of the solute is fixed at c_p at distances $>100 \mu$ m. The distance 100 μ m was chosen as a minimum achievable perfusion distance, however, it is effectively infinite insofar as the concentration profile does not significantly change if the perfusion plane is moved to infinity, so perfusion is irrelevant to our analysis. Because the pipette tip and cell membrane are the primary barriers to diffusion, the concentration in the cell is approximately spatially uniform, whereas a concentration gradient in the pipette is required to drive the flux j into the cell.

tration profile within the cell is assumed to be approximately uniform (Oliva et al., 1988; Mogul et al., 1989). Concentration gradients within the cell can be estimated from Fick's law: membrane fluxes on the order of 1 μ A/cm² require a maximum intracellular concentration change of ~ 1 M over 10 μ m for small monovalent solutes like sodium or potassium. In contrast, owing to the diffusion limitation of the pipette tip, a much larger concentration gradient may form between the bulk pipette solution and cell whenever a substance is transported across the cell membrane.

In all of the analysis that follows, we will consider either a free intracellular solute or one that is mostly bound to a mobile buffer. In the latter situation the flux into the cell from the pipette will be primarily in the buffered form, whereas the transmembrane flux is the unbuffered solute. As shown in the Appendix, both fluxes depend on the total concentration of solute in the cell, so

the concentration c_i is the total of free plus buffered solute.

Steady state diffusion

The goal of the steady-state analysis is to relate the bulk pipette concentration, c_p , to the intracellular concentration, c_i , in terms of experimentally measurable parameters. Assume the net transmembrane transport rate of an intracellular solute is j (mol/s). At steady state, the total flux from the pipette into the cell must equal the net membrane transport.

$$j = -A(x)D \frac{dc}{dx} \quad (\text{mol/s}), \quad (1)$$

where D (cm²/s) is the diffusion coefficient for c , and $A(x)$ (cm²) is the cross-sectional area of the pipette shank.

Eq. 1 can be integrated to obtain

$$\frac{j}{D} \int_{-a}^0 \frac{dX}{A(x)} = - \int_{c_p}^{c_i} dc, \quad (2)$$

where c_p (mol/cm³) is the bulk pipette concentration and a (cm) is the perfusion distance, which can be infinite in the absence of perfusion (Oliva et al., 1988). It is necessary to make some assumption on the geometry of the shank to complete the integration, however, an alternative approach is to write the integral in terms of the pipette shank resistance, R_p .

$$R_p = \rho \int_{-a}^0 \frac{dx}{A(x)} \quad (\Omega), \quad (3)$$

where ρ (Ω cm) is the resistivity of the solution filling the pipette. Substituting Eq. 3 into Eq. 2 and solving for c_i yields

$$c_i = c_p - \frac{jR_p}{D\rho} \quad (\text{mol/cm}^3). \quad (4)$$

Eq. 4 treats j as the independent parameter in setting c_i , whereas in actuality the rate of net transport depends on c_i and the membrane surface area of the cell. However, if the rate of transport can be experimentally measured, Eq. 4 allows one to correct for differences between c_p and c_i . Fig. 2 illustrates the steady-state value of c_i as a function of the net membrane flux. The value of c_i can be either greater or less than c_p , depending on whether the net flux is inward or outward. In general, the net flux will be inward when the concentration of free solute in the pipette is less than the normal resting value in the cell, and vice versa.

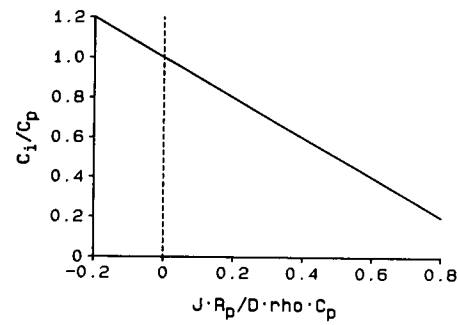


FIGURE 2 The steady-state relationship between intracellular concentration, c_i , bulk pipette concentration, c_p , and net membrane flux, j . This relationship is described by $c_i = c_p - j R_p / D\rho$, where the ratio of pipette resistance to resistivity, R_p/ρ , is a geometric factor that describes the pipette tip and D is the diffusion coefficient of the solute. When $j = 0$, the pipette concentration is the same as the normal resting intracellular concentration.

Steady-state electrodiffusion

Assume a holding current, i_h , is applied to voltage clamp the cell, where outward transmembrane current is defined as positive. There will be a voltage gradient within the pipette and if a substance is charged, its movement will be affected by this gradient. However, we will show that this is a small effect in most experimental situations so the primary limitation is diffusion across the pipette tip.

$$i_h = - \frac{A(x)}{\rho} \frac{d\psi}{dx} \quad (A) \quad (5)$$

$$j = -A(x)D \left[\frac{dc}{dx} + \frac{Fz}{RT} c \frac{d\psi}{dx} \right]. \quad (6)$$

Substituting Eq. 5 into Eq. 6 yields a first-order linear differential equation, which can be solved to obtain

$$c_i = c_p \exp \left(\frac{FzR_p i_h}{RT} \right) - \frac{RTj}{DFz\rho i_h} \left[\exp \left(\frac{FzR_p i_h}{RT} \right) - 1 \right]. \quad (7)$$

The term $R_p i_h$ (V) represents the voltage drop in the pipette. This should generally be smaller than RT/F in which case we make the approximation

$$c_i = c_p \left(1 + \frac{FzR_p i_h}{RT} \right) - \frac{jR_p}{D\rho}. \quad (8)$$

This result can be compared with Eq. 4 for diffusion in the absence of a voltage gradient. The correction, which depends on the voltage drop in the pipette divided by RT/F , is in most instances negligible, so the primary limitation of the technique is indeed the rate of diffusion of substances through the pipette tip.

Transient equations

Results concerning the time course of concentration changes require initial conditions that are appropriate for a specific experiment. However, before considering specific experiments, it is useful to write down general equations, which we can use to describe any experiment. In this section, we present these general equations.

The rate of change in c_i depends on the rate of entry via the pipette (Oliva et al., 1988) minus the solute flux across the membrane:

$$\frac{dc_i}{dt} = \frac{1}{\tau_p} (c_p - c_i) - \frac{1}{V_i} j \quad (\text{mol/cm}^3 \text{ s}). \quad (9)$$

For most cells, τ_p is in the range of 10–100 s.

$$\tau_p = R_p V_i / D\rho. \quad (10)$$

If one can experimentally measure j , the intracellular concentration can be computed.

$$c_i(t) - c_p = [c_i(0) - c_p] e^{-t/\tau_p} - \frac{1}{V_i} \int_0^t e^{-(t-s)/\tau_p} j(s) ds. \quad (11)$$

Whenever the time of the experiment is brief, so that $t \ll \tau_p$, the term $e^{-t/\tau_p} \approx 1$ and the pipette has essentially no influence on the change in concentration. For example, a voltage clamp experiment of voltage dependent ion channels would probably be too fast for the pipette to be effective.

We frequently use a linearized model of transport, in which j is expanded in Taylor series about $c_i = c_o$, where c_o is some fixed value concentration in the cell. The equations for transport then depend on the parallel combination of two time constants. One time constant, τ_p , represents the time for solute to move from pipette to cell, and the other, τ_T , represents the time for transport to move solute out of the cell.

The linearized equation is

$$\frac{dc_i}{dt} = \frac{1}{\tau_p} (c_p - c_i) - \frac{1}{\tau_T} (c_i - \bar{c}_o). \quad (12)$$

We define the flux when $c_i = c_o$ as

$$j_o = j(c_o) \quad (13)$$

then

$$\bar{c}_o = c_o - j_o \left/ \frac{dj_o}{dc_i} \right. \quad (14)$$

and

$$\tau_T = V_i \left/ \frac{dj_o}{dc_i} \right. \quad (15)$$

If $j_o \neq 0$, we can define normalized concentrations

$$C_i = \frac{c_i - \bar{c}_o}{c_o - \bar{c}_o}, \quad C_p = \frac{c_p - \bar{c}_o}{c_o - \bar{c}_o} \quad (16)$$

and

$$j(t) = j_o C_i(t). \quad (17)$$

The equation governing C_i is

$$\frac{dC_i}{dt} = \frac{1}{\tau_p} (C_p - C_i) - \frac{1}{\tau_T} C_i. \quad (18)$$

Eqs. 17 and 18 show that knowledge of just a few experimentally accessible parameters is sufficient to predict both the flux and the change in intracellular concentration.

Time constant of equilibration

The effect of membrane transport on the time course for equilibration of a solute between a patch pipette and cell may not be intuitively obvious. Consider the flux of sodium, for example. Assume we form a patch and rupture the membrane at $t = 0$. We will examine separately two situations: (a) the membrane is completely impermeable to sodium; (b) the Na/K pump responds to intracellular sodium. We will show that the time constant for equilibration is always more rapid when there is a transmembrane flux of the solute, regardless of whether the flux is inward or outward or whether the pipette concentration is greater or less than $c_i(0)$.

We form a patch and rupture the membrane at $t = 0$, then wait for the concentration in the pipette to equilibrate with the intracellular compartment. If the substance is impermeant, as in case 1, then

$$\begin{aligned} \frac{dc_i}{dt} &= \frac{1}{\tau_p} (c_p - c_i) \\ c_i(0) &= c_o \end{aligned}$$

and

$$c_i(t) - c_o = (c_p - c_o)(1 - e^{-t/\tau_p}). \quad (19)$$

If we assume there is membrane transport of sodium, as in case 2, and that we are initially in steady state (i.e., $j = 0$ at $c_i = c_o$), then from Eq. 12

$$c_i(t) - c_o = \frac{c_p - c_o}{1 + \tau_p/\tau_T} (1 - e^{-t/\tau}), \quad (20)$$

where

$$\tau = \tau_p / (1 + \tau_p/\tau_T). \quad (21)$$

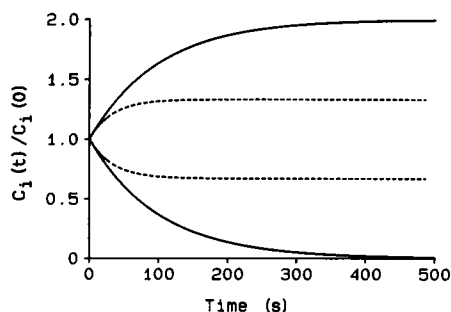


FIGURE 3 The time course of the intracellular concentration change. The solid lines are calculated assuming an impermeable cell membrane, and the dashed lines a permeable cell membrane. The bulk pipette concentration is assumed to be twice the resting intracellular concentration in the upper 2 curves, and zero in the lower 2 curves. The presence of membrane transport always accelerates the time to steady state but reduces the magnitude of the change in intracellular concentration.

The predictions of Eqs. 19 and 20 are graphed in Fig. 3 for $\tau_T = \tau_p$ and $c_p = 2c_o$ or $c_p = 0$. The solid lines represent the concentration changes in the absence of transport and the dashed lines in its presence. We have assumed that the passive inward leak is essentially constant, so the time course of concentration change reflects either stimulation or inhibition of the active transport component. In Fig. 3, the initial rate of change in concentration depends only on the pipette, but the final change is always reduced by transport, so the time constant is reduced. When pipette sodium is elevated, the pump is stimulated to extrude it. When pipette sodium is below normal, the pump is inhibited, however, in the presence of a constant inward background leak, the inward transmembrane flux of sodium is effectively stimulated. Thus, the change in intracellular sodium is reduced and so is the time constant for equilibration, regardless of whether the membrane flux is net inward or outward.

Because j varies as the surface area of the cell, the time constant τ_T (Eq. 15) varies inversely with the cell's surface to volume ratio, whereas τ_p (Eq. 10) varies in proportion to cell volume. Thus, the time to steady state in very small cells will depend primarily on τ_p , whereas very large cells will depend primarily on τ_T .

RESULTS

In this section we will examine experiments using the whole cell patch clamp to study the Na/K ATPase and Na/Ca exchange in the heart. We will use nonlinear models of these transporters so the results are computed numerically, however, our computed results are compared with the linearized, approximate results presented in Theory.

The Na/K pump

One of the most important factors in the regulation of sodium pump activity is its response to changes in intracellular sodium. If we attempt to characterize the dependence of transport rate on $[Na]_i$, by using the whole cell patch clamp technique and perfusing the pipette with various values of $[Na]_p$, the effectiveness of the pump will limit the change in $[Na]_i$.

We assume that 3 sodium are transported for 2 potassium and that each binding site for a particular ion is independent and identical.

$$j_T = \bar{j}_T \left(\frac{[K]_e}{[K]_e + K_K} \right)^2 \left(\frac{[Na]_i}{[Na]_i + K_{Na}} \right)^3 \quad (22)$$

The dissociation constant for intracellular sodium is selected to give a half-max binding at $[Na]_i = 10$ mM, in accordance with data reported by Nakao and Gadsby (1989). The remaining transport parameter values are rough estimates taken from our own data from guinea pig myocytes (Gao et al., 1990a, b).

$$R_p = 4 \text{ M}\Omega$$

$$K_{Na} = 2.6 \text{ mM}$$

$$K_K = 2.1 \text{ mM}$$

$$[K]_e = 5 \text{ mM},$$

and

$$\bar{j}_T = 8.9 \text{ fmol/s}.$$

The passive leak of sodium into the cell is calculated using the Goldman, Hodgkin, Katz equation, which assumes a constant field within the membrane.

$$j_L = \omega_{Na} \frac{F\psi_m}{RT} \frac{[Na]_i - [Na]_e e^{F\psi_m/RT}}{1 - e^{F\psi_m/RT}}, \quad (23)$$

where the membrane permeability, $\omega_{Na} = 3.2 \times 10^{-12}$ cm³/s was chosen such that $j_T = -j_L = 1.5$ fmol/s at $[Na]_i = 6$ mM and at $\psi_m = -80$ mV.

In Fig. 4 we have plotted the actual binding curve for intracellular sodium (*solid line*) and the data (*squares*) that one would obtain using a 4-M Ω patch pipette to record the membrane current as a function of pipette sodium. The effect of intracellular depletion is to reduce and linearize the apparent binding curve in relation to the actual binding. The actual and apparent binding curves cross at the normal resting value of intracellular sodium, where $j = 0$. Thus, the ouabain blockable current at the resting value of $[Na]_i$ is also a measure of the leak. If we assume j_L is independent of $[Na]_i$, then there is enough experimental information to correct the simulated data in Fig. 4 using the relationship in Fig. 2, and obtain the

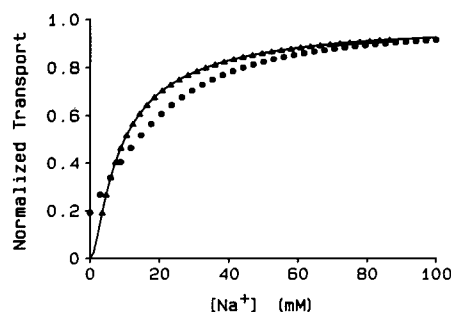


FIGURE 4 The sodium dependence of the Na/K ATPase. The solid line represents the actual dependence of the pump on intracellular sodium. The open squares are a simulation of the observed pump current as a function of pipette sodium. The observed curve is more linear and less steep than the actual, owing to differences in intracellular sodium and pipette sodium. The leak of sodium into the cell is calculated using the constant field assumption, Eq. 23, which varies slightly with changes in $[Na]_i$. The filled diamonds are calculated by shifting the observed points along the abscissa in accordance with Eq. 4, assuming a constant leak so that j is the observed flux minus a constant. Numerical simulations were performed using an IBM PC with an inboard 386/P were written in Fortran 77. Programs for integration of nonlinear differential equations, root finding and function maximum finding were taken from Press et al. (1986).

triangles in Fig. 4. The small difference between the triangles and the actual binding curve is due to the variation in j_L , which is calculated using Eq. 23 in the simulated data but is assumed to be a constant, given by its resting value, in the correction.

The Na/Ca exchanger

The Na/Ca exchanger is thought to move 3 Na^+ for 1 Ca^{++} . It most often uses the energy in the sodium gradient to extrude calcium from the cell, however, it may reverse direction and transport calcium into the cell during part of the plateau phase of the cardiac action potential (Noble, 1986). It is the primary transport system for eliminating the Ca^{++} which enters during the cardiac action potential, so it is very responsive to changes in intracellular Ca^{++} and is capable of rapidly altering $[Ca]_i$.

Kimura et al. (1987) present an elegant set of experiments in which they characterize many aspects of this important transporter. In their study, they noted changes in flux that were most probably due to changes in intracellular concentration. Kimura et al. described these changes as local accumulation/depletion of Ca^{++} just inside the membrane, but given the slow time scale, they are most likely related to a more global phenomenon, probably accumulation/depletion of total intracellular calcium, which is mostly bound to EGTA in their experiment. In the Appendix, we show that if local accumula-

tion/depletion occurs, it will be within 1 μm of the membrane and will develop within a few milliseconds. Moreover, the flux of calcium reported in Kimura et al. (1987) is on the order of 10^{-15} mol/s. To provide a flux of this magnitude from the pipette, we require a concentration difference of $c_p - c_i \approx 1.0$ mM. Because free calcium is on the order of 10^{-7} M, the required flux is obviously being delivered by the buffered calcium, whose concentration is in the millimolar range. The concentration of relevance is therefore that of buffered calcium, $c_i = [Ca-EGTA]_i$, and the reported time constant is for changes in c_i .

In these experiments, both extracellular sodium and intracellular calcium are changed, so we explicitly consider the effect of each. However, the time course of depleting total cellular calcium appears exponential, suggesting that the linearized model (Eq. 17) is an adequate description of their experiment. Thus, we assume

$$j = j_0 P_e^3 C_i(t) \quad (24)$$

$$P_e = \frac{[Na]_e}{[Na]_e + K_{Na}} \quad (25)$$

and

$$\frac{dC_i}{dt} = \frac{1}{\tau_p} (1 - C_i) - \frac{1}{\tau_T} P_e^3 C_i \quad (26)$$

$$C_i(0) = 1,$$

where τ_T and τ_p are defined in Eqs. 10 and 15, but we specify τ_T at $P_e = 1$. For an arbitrary $[Na]_e$, where $P_e \neq 1$, the actual time constant for transport becomes τ_T/P_e^3 .

Kimura et al. (1987) measured the time course of intracellular depletion by voltage clamping to the reversal potential of the transporter where $j \approx 0$, then stepping to some test voltage and recording the flux.

In this experiment, they used $[Na]_e = 140$ mM, which is close to saturating (see Fig. 5 E). To estimate some of the parameters of the model, we assume $P_e \approx 1$ at $[Na]_e = 140$ mM. Then the flux measured by Kimura et al. is described by

$$j(t) = j_\infty + (j_0 + j_\infty)e^{-t/\tau}$$

$$j_\infty = \frac{j_0}{1 + \tau_p/\tau_T},$$

where τ is given by Eq. 21. From their data, we can measure

$$j_0 = 8.1 \text{ p mol/s}$$

$$j_\infty = 1 \text{ p mol/s}$$

$$\tau = 12 \text{ s.}$$

For a typical pipette of 4 M Ω resistance and a cardiac ventricular myocyte of volume 2×10^{-8} cm³, the pipette

time constant will be 100 s. Using this value of τ_p , we can calculate the remaining parameters.

$$\tau_p = 100 \text{ s}$$

$$\tau_T = 14 \text{ s.}$$

One of the points of the experiments described in Kimura et al. (1987) was to measure the dependence of the exchanger $[Na]_e$ (to determine P_e^3 in our model). To do so, they recorded the peak current when their bath was changed from $[Na]_e = 0$ to an arbitrary $[Na]_\infty$. If the bath change is instantaneous, the initial flux would be $j_0 P_e^3$, where P_e is evaluated at $[Na]_\infty$. However, their bath change appears to have a time constant, τ_b , that is comparable to their rate of intracellular depletion. Thus,

$$[Na]_e = [Na]_\infty (1 - e^{-t/\tau_b}), \quad (27)$$

where

$$\tau_b \approx 12 \text{ s.}$$

The probability of binding three extracellular sodium ions now follows a time course that is dictated by the bath exchange (Eq. 27). We assume the rate of binding Na^+ is fast in comparison to the bath change, so we compute $P_e(t)$ from Eqs. 25 and 27. Thus,

$$j(t) = j_0 P_e^3(t) C_i(t),$$

where $C_i(t)$ is numerically calculated by integrating Eq. 26.

Fig. 5, A–D illustrate the predicted fluxes when the extracellular bath is changed from $[Na]_e = 0$ to $[Na]_\infty = 140, 70, 35$, and 17.5 mM, respectively. These computations are similar to the fluxes recorded by Kimura et al. (1987) and graphed in Fig. 8 of that paper. We predict somewhat more depletion than shown in Fig. 8 of Kimura et al. but our calculation uses a time constant that is obtained under slightly different conditions, and a pipette resistance of $4 \text{ M}\Omega$, which may be higher than that used in their particular experiment.

We define T as the time of peak flux. The normalized peak flux is

$$\frac{j(T)}{j_0} = P_e^3(T) C_i(T). \quad (28)$$

Kimura et al. (1987) assumed that $j(T)/j_0 = P_e^3$. This assumption is accurate when the bath change is rapid in comparison to intracellular depletion, but becomes increasingly in error as τ approaches τ_b . In Fig. 5 E, we plot: (a) $P_e^3([Na]_\infty)$ vs. $[Na]_\infty$; and (b) $j(T)/j_0$ vs. $[Na]_\infty$. Curve 2 falls significantly below curve 1 at most values of $[Na]_\infty$. This is due to two factors: (a) The bath sodium concentration at the time of peak flux is less than $[Na]_\infty$, due to the slow bath exchange; (b) The intracellular concentration

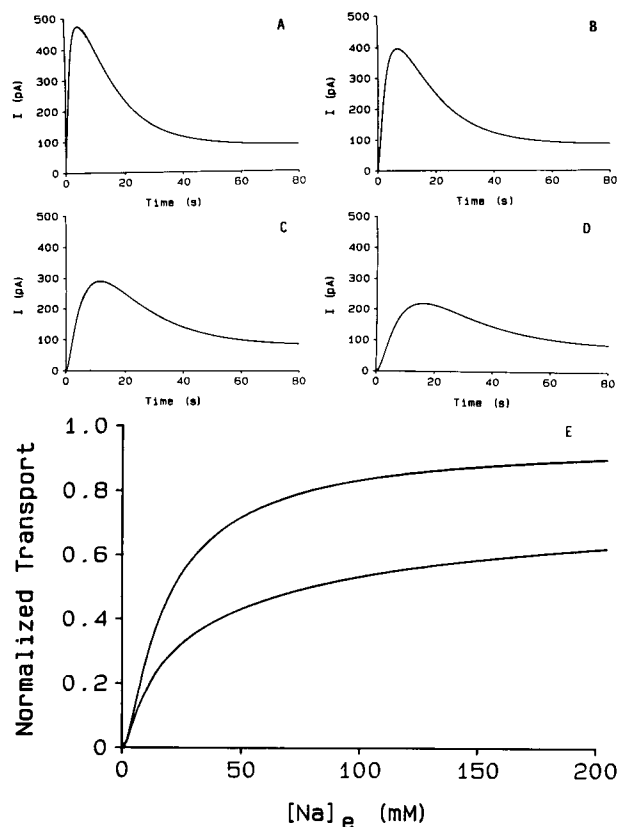


FIGURE 5 Na/Ca exchange currents and binding of extracellular sodium. A–D illustrate the time course of current generated by the exchanger, starting from the same initial conditions with zero initial current owing to zero initial extracellular sodium. The exchanger is assumed to be turned on by changing the bath sodium with a time constant $\tau_b = 12$ s. The final bath sodium is: (A) 140 mM; (B) 70 mM; (C) 35 mM; (D) 17.5 mM. E illustrates the actual and observed binding curves for extracellular sodium. The upper curve is the actual binding calculated from Eq. 25. The lower curve represents the peak current as a function of the final bath sodium. The half-max of the actual binding curve occurs at 20 mM, whereas the peak current yields a half-max at 70 mM. The errors in using the peak current to estimate $[Na]_e$ binding are due to two factors: (a) the bath sodium has not reached its final value at the time of the peak, and (b) the intracellular calcium is depleted at the time of peak.

$C_i(T)$ at the time of peak flux has dropped from its initial value, due to intracellular depletion of total calcium. Indeed, it appears that the correct half maximum should be ~ 20 mM, which is 3.5 times lower than that calculated by Kimura et al. using the measured peak flux. For the corrected binding curve, the dissociation constant in Eq. 25 is

$$K_{Na} = 5 \text{ mM,}$$

$$P_e^3 = 0.5 \text{ at } [Na]_e = 20 \text{ mM.}$$

We adjusted K_{Na} to make the peak flux vs. $[Na]_e$ curve in Fig. 5 E appear similar to that reported by Kimura et al.

As mentioned above, the calculations in Fig. 5 utilize parameters measured in different experiments on different cells, so the corrected binding curve may not be very accurate. Nevertheless, it demonstrates that the effects are significant and a correction is important.

DISCUSSION

We have extended the findings of Oliva et al. (1988) to the study of membrane transport and demonstrated that concentrations of transported substances will differ between the pipette and the cell under most conditions. This discrepancy between pipette and cell concentrations can lead to incorrect estimates of the transport properties of the cell membrane. We analyzed two membrane transporters, the Na/K pump and Na/Ca exchange in ventricular cells of the mammalian heart.

Na/K pump

Our study of the sodium pump focused on the relationship of the transport rate to the pipette sodium concentration. We demonstrated that for conservative values of the pipette resistance and pump flux in a ventricular myocyte, the relationship between pipette sodium and transport deviated significantly from the relationship between internal sodium and transport. The former shows less saturation below 100 mM pipette sodium, with a half saturation at ~15 mM, whereas the latter had a half saturation value of 10 mM. The initial studies examining the Na⁺ dependence of the Na/K pump showed even less saturation than our simulated data (Gadsby et al., 1985), whereas later studies aimed at this particular concern were able to demonstrate saturation with a half-maximum at near 10 mM pipette sodium by using very low resistance pipettes (Nakao and Gadsby, 1989).

More recently a number of important studies have concerned the current voltage relationship of the Na/K pump and the properties of the voltage dependent step in Na⁺ transport (Gadsby and Nakao, 1989). The qualitative conclusions of these studies remain unaltered by the difficulties of the patch-clamp technique, however, it is less certain that the quantitative estimates are entirely correct. The relationship between intracellular sodium and membrane potential will depend on the transport rate of the Na/K pump and the inward background current, which will also determine these fluxes.

Time constant of equilibration

Pusch and Neher (1988) measured the time constants for intracellular equilibration of a number of solutes that

were perfused in patch pipettes. Their results for impermeant solutes could be accurately described using the results of Oliva et al. (1988), where τ_p (Eq. 10) gave the time constant for the cell and pipette to equilibrate.

The time constants for Na⁺ or K⁺ equilibration, however, were several times faster than predicted by the Oliva et al. analysis. In Theory, we used a linearized approximate model to demonstrate that membrane transport will always speed up the time to steady state. In Oliva et al. (1988) we suggested that the Na/K pump might have sped up the time to steady state for these ions. However, a quantitative analysis suggests the Na/K pump in relatively small chromaffin cells used by Pusch and Neher would not produce enough flux to be responsible for the more rapid time constants. The observation in Fig. 3 that membrane pumps can speed the equilibration time applies to any membrane flux, either passive or active, so Na⁺ or K⁺ membrane channels also shorten the time to steady state. If a solute is diffusing from pipette to cell, an outward membrane flux hastens the time to steady state by reducing the steady-state change, as shown in Fig. 3, whereas an inward membrane flux increases the rate of accumulation.

Na/Ca exchange

The intracellular calcium concentration is normally low, so consequently it presents some unique experimental difficulties. The first is in loading the cell with a desired level of calcium. If the pipette contains a free, unbuffered calcium concentration that is below 10 μ M, Neher (1988) showed that the time for equilibration of the cell and pipette will be extremely slow, owing to the presence of fixed intracellular buffers (e.g., myofilaments, sarcoplasmic reticulum, nuclei, and mitochondria). In the Appendix, we calculate that the time constant for equilibration of free calcium may be thousands of times slower than that for sodium. The means to avoid this problem is to load the pipette with a high (millimolar) concentration of buffered calcium, so diffusion from pipette to cell is in the form of calcium bound to a mobile buffer. This will create a large enough flux of total calcium into the cell to rapidly equilibrate with fixed intracellular buffers. Mobile buffers, however, have unknown effects on the binding reaction of intracellular calcium with the Na/Ca exchange protein.

As described in the Appendix, when mobile calcium buffers are present, two reactions can occur at the membrane-myoplasm interface: (a) free calcium can bind to the Na/Ca exchange protein. (b) Buffered calcium can be directly transferred to the transport protein. The affinity of the transport protein for a free calcium ion is higher than for one bound to a buffer, however, buffered calcium is thousands of times more plentiful than free

calcium, so reaction *b* is greatly favored by mass action. One or the other of these reactions will likely dominate, but we do not know which. Furthermore, as indicated in the Appendix, there are special problems associated with each reaction.

If reaction (*a*) dominates, there may be rapid local depletion of calcium within 1 μm of the membrane. If reaction (*b*) dominates, local depletion will be negligible. However, the transfer of calcium from a mobile buffer directly to the exchange protein will depend on rate constants that are not normally associated with calcium extrusion by the exchanger.

Experiments on Na/Ca exchange have not been executed with sufficient time resolution to detect a rapid decline due to local depletion. Kimura et al. (1987) report that their conclusions did not depend on intracellular concentrations of EGTA between 4 and 40 mM, as long as free calcium was maintained constant. Ehara et al. (1989) examined the effects of different concentrations of EGTA and BAPTA. They found that the time constant for the decay of the Na/Ca exchange current increased with increased buffer concentration. This observation is predicted in the Appendix, Eq. A27, which describes the time constant for depletion of intracellular buffered calcium. The evidence for choosing between reaction (*a*) or (*b*) is not particularly compelling. However, the calcium and sodium fluxes reported by Kimura et al. (1987) or Ehara et al. (1989) were surprisingly large if free calcium (10^{-7} M) is the source. They measured peak currents that were 1–2 $\mu\text{A}/\text{cm}^2$. Na/K pump currents are the same order of magnitude, whereas free Na^+ and K^+ are 10,000 times more plentiful than free Ca^{++} . Perhaps the relatively high concentration of mobile buffered calcium enhances the flux through the Na/Ca exchanger. Clearly, there are interesting questions yet to be answered.

APPENDIX

The effect of buffering

Diffusion of ions present at low free concentration can be greatly modified by mobile and immobile buffers. These effects, with regard to intracellular diffusion of hydrogen ion, are discussed in Junge and McLaughlin (1987) and Irving et al. (1990). Similar effects are expected for calcium (Neher, 1988). The interaction of calcium or hydrogen (Kasianowicz et al., 1987) with a membrane transport system will also be modified by buffers. The purpose of this appendix is to examine the effects of mobile and immobile buffers on the transport and intracellular concentration of calcium during whole cell patch clamp studies of Na/Ca exchange in heart cells.

Fixed buffers

Calcium has several intracellular storage sites that buffer changes in free concentration. The majority of these sites are not free to diffuse

from the cell (for example, mitochondria, sarcoplasmic reticulum, myofilaments, and nuclei), so diffusion of free calcium from a patch pipette into a muscle cell must fill or come to equilibrium with these fixed buffers. Such sites have the capacity to absorb the equivalent of millimolar concentrations of free calcium, although they are saturable, and they can equilibrate with free concentrations in the 1–10 μM range. As a first approximation, we will model this group of intracellular sites as a simple buffer:

$$[SCa]_i = \frac{[S]_T [Ca]_i}{K_s + [Ca]_i}, \quad (\text{A1})$$

where $[S]_T$ (millimolar) is the total capacity, $[SCa]_i$ (millimolar) is the amount of calcium in the stores (each referred to an equivalent concentration of free calcium), $[Ca]_i$ (micromolar) is free intracellular calcium and K_s (micromolar) is an effective dissociation constant.

Diffusion of free calcium from a pipette into a cell will increase both free calcium and calcium stored in these intracellular sites. The differential equation describing accumulation/depletion of intracellular calcium is, therefore:

$$\frac{d[Ca]_i}{dt} + \frac{d[SCa]_i}{dt} = \frac{1}{\tau_p} ([Ca]_p - [Ca]_i) - \frac{1}{V_i} j. \quad (\text{A2})$$

If the time for diffusion is slow in comparison to the rate constants for filling the intracellular sites, the storage sites will remain near equilibrium, which is described by Eq. A1. Differentiating Eq. A1 and substituting into the linearized version of Eq. A2 yields

$$\frac{d[Ca]_i}{dt} = \frac{\beta_s}{\tau_p} ([Ca]_p - [Ca]_i) - \frac{\beta_s}{\tau_T} ([Ca]_i - [\overline{Ca}]_o), \quad (\text{A3})$$

where

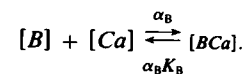
$$\beta_s = 1 \left/ \left[1 + \frac{[S]_T/K_s}{(1 + [Ca]_i/K_s)^2} \right] \right. \quad (\text{A4})$$

The buffer capacity, β_s , as defined in Eqs. A3 and A4, is approximately the change in free calcium per unit change in total calcium. For free intracellular calcium in the micromolar range, β_s is likely to be on the order of $\beta_s \approx 10^{-3}$. The time constant for the pipette to come to a steady state with the cell will therefore be extremely slow ($10^3\tau$, where $\tau = \tau_p/1 + \tau_p/\tau_T$).

Mobile buffers

Because of the above described limitation, one usually controls intracellular calcium by perfusing the pipette with a mobile calcium buffer (Neher, 1988). Buffered calcium, $[BCa]$, is in the millimolar range, whereas free calcium, $[Ca]$, is in the sub micromolar range. Thus, there is a relatively large flux of buffered calcium from the pipette into the cell, where the mobile buffer and fixed buffers come to equilibrium. In this situation, we will show that the time to steady state is probably not significantly affected by fixed buffers. However, when membrane transport of calcium is significant, interactions of buffered calcium with the transport protein and local depletion of free calcium may both occur.

Within the cell and pipette, the buffer reaction is



We will assume that changes in bulk intracellular concentration are slow

in comparison to the rate of binding, hence,

$$[Ca] = K_B \frac{[BCa]}{[B]} \quad (A5)$$

Furthermore, if the diffusion coefficients of B and BCa are similar, then any increase in free intracellular buffer, $[B]_i$, corresponds to an equivalent decrease in the intracellular concentration of buffer-calcium complex, $[BCa]_i$.

$$\frac{d[BCa]_i}{dt} \approx - \frac{d[B]_i}{dt} \quad (A6)$$

The equation describing the total change in intracellular calcium is

$$\frac{d[BCa]_i}{dt} + \frac{d[Ca]_i}{dt} + \frac{d[SCa]_i}{dt} = (j_{in} - j)/V_i \quad (A7)$$

In this situation, the flux from the pipette, j_{in} , is almost entirely buffered calcium. Moreover, free calcium is a negligible component of the total balance so we can ignore $[Ca]_i$ in Eq. A7 and eliminate $[SCa]_i$ using Eqs. A1, A5, and A6. The result is:

$$\frac{d[BCa]_i}{dt} = \beta_S (j_{in} - j)/V_i \quad (A8)$$

where β_S is now defined by

$$\beta_S = 1 / \left[1 + \frac{[S]_T/K_S}{[B]_T/K_B} \left(\frac{1 + [Ca]_i/K_B}{1 + [Ca]_i/K_S} \right)^2 \right] \quad (A9)$$

and where $[B]_T = [BCa]_i + [B]_i$. Although it is difficult to know precisely the values of the parameters in Eq. A9, for buffers such as EGTA, whose $K_B = 10^{-7}$ M, the ratio of K_S/K_B is probably >1 , so for a total buffer concentration of greater than a few millimolar, $\beta_S \approx 1$. We will assume $\beta_S \approx 1$ in what follows.

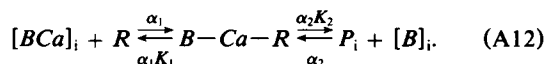
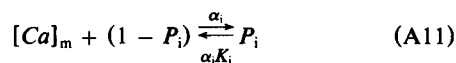
The flux of calcium from the pipette is almost entirely in the buffered form because buffered calcium is three orders of magnitude more abundant than free. Thus,

$$\frac{1}{V_i} j_{in} = \frac{1}{\tau_p} ([BCa]_p - [BCa]_i), \quad (A10)$$

and in the text of this paper, when we are considering a buffered ion such as calcium, $c_i = [BCa]_i$.

Membrane/calcium interactions

The final step is to relate the membrane transport to the concentration of buffered calcium in the cell. At the inside surface of the membrane, the transport protein can pick up calcium through two paths.



P_i represents the fraction of the total number of transport proteins with their calcium binding site filled, and $[Ca]_m$ is the calcium concentration just inside the membrane. If Reaction A11 dominates, there will be local depletion of calcium just inside the membrane, as shown in Fig. A1, and

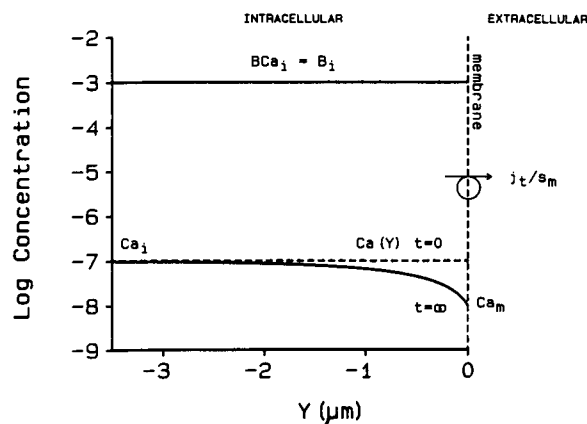


FIGURE A1 The spatial dependence of intracellular calcium just inside the cell membrane. The cell membrane is at $y = 0$, where calcium is extruded at a rate j_t/S_m (mol/cm² s). When mobile buffering is inadequate, calcium just inside the membrane, $[Ca]_m$, is significantly less than bulk intracellular calcium, $[Ca]_i$. The depletion occurs within 1 μ m of the membrane and develops with a time course of <1 m s. Mobile buffered calcium, $[BCa]_i$, is approximately spatially uniform (gradients are in the micromolar range, whereas concentration is in the millimolar range). The buffer acts as a shuttle bringing calcium to the membrane, then empty buffer, $[B]_i$, diffuses away from the membrane and binds a new calcium ion. Thus, the greater the concentration of mobile buffer, the less the local depletion of calcium. However, total buffer can deplete over a time of a few seconds, owing to the diffusion limitation of the pipette tip. Moreover, calcium can be delivered directly to the calcium transport protein without disassociating from the buffer into the free state. The direct transfer of calcium from buffer to membrane protein involves binding constants for each system.

in this reaction layer the buffer will be out of equilibrium. If Reaction A12 dominates, then local depletion is negligible; because this is the simpler situation, we will first consider Reaction A12.

Buffered calcium/membrane interaction

We assume that the time constant for changes in $[BCa]_i$ is slow in comparison to the rate of binding, so P_i is determined by an equilibrium analysis. The analysis can be further simplified by assuming that the middle state is in low occupancy. This implies $[BCa]_i/K_1 \gg 1$ and $[B]_i/K_2 \gg 1$. Then

$$P_i = \frac{[BCa]_i}{[BCa]_i + \frac{K_1}{K_2} [B]_i} \quad (A13)$$

This can also be written in terms of free calcium by using Eq. A5.

$$P_i = \frac{[Ca]_i}{[Ca]_i + \frac{K_1}{K_2} K_B} \quad (A14)$$

Thus, changing the amount of pipette buffer and total calcium, such that free calcium remains constant, results in no change in binding as described by Kimura et al. (1987). However, the binding constant depends on which buffer is used.

We assume that there is just one calcium binding site per transporter, hence the flux due to transport is

$$j_T = \bar{J}_T P_e^3([Na]_e) \frac{[Ca]_i}{[Ca]_i + \frac{K_1}{K_2} K_B}. \quad (A15)$$

Free calcium/membrane interaction

The second limiting possibility is that Reaction A11 dominates. As described in the text and in Neher (1986) intracellular concentration gradients of a few micromolar are sufficient to drive the fluxes, hence the values of $[BCa]_i$ and $[B]_i$ will be approximately uniform in the cell, as shown in Fig. A1, but a gradient in free calcium will form just inside of the membrane.

This situation was analyzed by Neher (1986) so we will attempt to make just a few general points. (a) The reaction layer, where free calcium has depleted, is $<1 \mu\text{m}$ thick. (b) The local gradient will form with a time constant $<1 \text{ ms}$. (c) Once formed, the reaction layer will maintain a pseudo steady state with the bulk cellular concentration of total calcium, which is approximately equal to $[BCa]_i$. Changes in $[BCa]_i$ occur on a time scale of seconds.

Define y (cm) as a local coordinate normal to the membrane with $y = 0$ at the inside surface of the membrane and y becomes more negative toward the center of the cell (see Fig. A1). The flux is assumed to be zero at $t < 0$, and suddenly switched on at $t = 0$.

The maximum value of j_T will occur at $t = 0$, whereas the minimum value will occur at $t = \infty$, when depletion has caused the calcium concentration just inside the membrane to fall to its minimum value of $[Ca]_m$. One should be aware, however, that $t \rightarrow \infty$ in just a few milliseconds, so $[Ca]_m$ may be time dependent, but it will be due to much slower processes. If we simplify the calculation by assuming that j_T is a constant, given by its minimum, final steady-state value, the time constant thus derived is an upper bound on the time of calcium depletion just beneath the membrane. The steady-state spatial distribution of calcium is accurately calculated because we define j_T as the final flux. Neher (1986) solved this diffusion/reaction problem for the conditions just described. In our nomenclature, his solutions are

$$[Ca](0, t) = [Ca]_i - \frac{\lambda j_T}{S_m D_{Ca}} \text{erf} \sqrt{t/\tau_m} \quad t \geq 0 \quad (A16)$$

$$[Ca](y, \infty) = [Ca]_i - \frac{\lambda j_T}{S_m D_{Ca}} e^{y/\lambda} \quad y \leq 0, \quad (A17)$$

where S_m (cm^2) is the total surface area of the cell, so the membrane flux density is j_T/S_m .

$$\tau_m = [Ca]_i / (\alpha_B K_B [BCa]_i) \quad (A18)$$

$$\lambda = \sqrt{D_{Ca} \tau_m}. \quad (A19)$$

Thus, the shorter the time constant, the shorter the length constant. For a fixed $[Ca]_i$, each will become shorter if the buffer concentration, $[BCa]_i$, is increased or if a different buffer with a higher off rate, $\alpha_B K_B$, is used. Define

$$\Delta[Ca] = [Ca]_i - [Ca]_m, \quad (A20)$$

where from Eq. A16 we find

$$[Ca]_m = [Ca]_i - \frac{\lambda j_T}{S_m D_{Ca}}. \quad (A21)$$

From the data in Kimura et al. (1987) for Na/Ca exchange, $[Ca]_i \sim 10^{-7} \text{ M}$ and $j_T/S_m \sim 10^{-11} \text{ mol/cm}^2\text{s}$, and because $\Delta[Ca] < [Ca]_i$, the maximum value of λ can be estimated from Eq. A20 and A21 with $\Delta[Ca] = 10^{-7} \text{ M}$ and $D_{Ca} \sim 10^{-5} \text{ cm}^2/\text{s}$, $\lambda < 10^{-4} \text{ cm}$

$$\lambda < 10^{-4} \text{ cm}$$

and from Eq. A19

$$\tau_m < 10^{-3} \text{ s}.$$

This demonstrates that depletion just beneath the membrane is highly localized and quite fast, much too fast to account for the depletion observed in Kimura et al. (1987) or Ehara et al. (1989). The concentration at the inner membrane surface, $[Ca]_m$, depends on bulk intracellular calcium, the length constant, and the rate of transport. But the rate of transport also depends on $[Ca]_m$, so we have the following nonlinear interdependence of binding and j_T .

$$j_T = \bar{J}_T P_e^3([Na]_e) \frac{[Ca]_m}{[Ca]_m + K_{Ca}}. \quad (A22)$$

Eq. A22 differs from Eq. A14 in two important regards: (a) binding of calcium in Eq. A22 depends on total buffer as well as free calcium, whereas, in Eq. A14 binding is not affected by total buffer if free calcium is constant. (b) The dependence of j_T on $[Na]_e$ in Eq. A22 is not a simple Langmuir binding curve, whereas in Eq. A14 it is. However, as the amount of buffer is increased, λ becomes shorter and $[Ca]_m \rightarrow [Ca]_i$ (see Eq. A21). For a sufficiently high buffer concentration, these differences will therefore disappear.

Transient changes in intracellular buffered calcium

As just demonstrated transient changes in free calcium just inside the membrane can make the analysis very complex. Nevertheless, when the buffer concentration is sufficiently high,

$$[Ca]_m \rightarrow [Ca]_i \quad (A23)$$

and either Eq. A15 or Eq. A22 can be written in the form

$$j_T = \bar{J}_T P_e^3([Na]_e) P_i([Ca]_i), \quad (A24)$$

where

$$P_i = \frac{[Ca]_i}{[Ca]_i + K} \quad (A25)$$

and

$$K = \begin{cases} K_1 K_B / K_2 & \text{for buffered calcium/membrane interaction} \\ K_{Ca} & \text{for free calcium/membrane interaction.} \end{cases} \quad (A26)$$

Given the above conditions, we will show that the time constant for depletion of intracellular buffered calcium depends on the initial concentrations of buffered calcium and free calcium. In all other regards, the analysis presented in Eqs. 9–18 of the text remains the same.

The rate of change in total intracellular calcium is well approximated by the rate of change in buffered calcium. In the absence of significant leak, this depends on influx from the pipette minus j_T (Eq. 8) but influx is

proportional to $[BCa]_p - [BCa]_i$, whereas j_T depends on $[Ca]_i$ (Eq. A24). Linearization of Eq. A24 around the initial concentration of buffered calcium, $[BCa]_o$, leads to an equation of the same form as Eq. 12 of the text. However, the interpretation of τ_T is slightly different. The time constant is calculated from the change in transport per change in buffered calcium. If the total intracellular calcium is c_i , then $c_i \approx [BCa]_i$ and

$$\tau_T = V_i \left/ \frac{dj_o}{dc_i} \frac{dc_i}{dCa_i} \right|_{c_o}.$$

In our model (Eq. A24), this gives

$$\tau_T = [BCa]_o V_i \left/ \left[\bar{J}_T P_c^3([Na]_e) \frac{K(K_B + [Ca]_o)[Ca]_o}{K_B(K + [Ca]_o)^2} \right] \right|. \quad (A27)$$

Thus, if the initial concentration of calcium is fixed but total buffer is increased, the time constant, τ_T , will be slower. If the initial concentration of calcium is changed, the effect on this time constant depends on the relative values of K and K_B .

We would like to thank Dr. George J. Baldo for his assistance with the figures, Betsy Bain for typing the manuscript, and Dr. Stuart McLaughlin for helpful discussion of the Appendix.

This work was supported by grants HL36075, EY 06391, HL28958, and HL20558.

Received for publication 15 January 1990 and in final form 16 May 1990.

REFERENCES

- Ehara, T., S. Matsuoka, and A. Noma. 1989. Measurement of reversal potential of Na—Ca exchange current in single guinea-pig ventricular cells. *J. Physiol.* 410:227–249.
- Gadsby, D., and M. Nakao. 1989. Steady-state current-voltage relationship of the Na/K pump in guinea pig ventricular myocytes. *J. Physiol.* 94:511–537.
- Gadsby, D., J. Kimura, and A. Noma. 1985. The isolated Na-K pump current: effects of changing external K, intracellular Na and ATP in internally dialysed single guinea-pig ventricular cell. *J. Physiol.* 358:55P.
- Gao, J., R. T. Mathias, I. S. Cohen, and G. J. Baldo. 1990a. Glycoside binding and ionic activation of ventricular Na/K. *Biophys. J.* 57:134a. (Abstr.)
- Gao, J., R. T. Mathias, I. S. Cohen, and G. J. Baldo. 1990b. Extracellular pH alters ventricular Na/K pump V_{max} . *Biophys. J.* 57:134a. (Abstr.)
- Irving, M., J. Malie, N. L. Sizto, and W. K. Chandler. 1990. Intracellular diffusion in the presence of mobile buffers. *Biophys. J.* 57:717–721.
- Junge, W., and S. McLaughlin. 1987. The role of fixed and mobile buffers in the kinetics of proton movement. *Biochim. Biophys. Acta.* 890:1–5.
- Kasianowicz, J., R. Benz, and S. McLaughlin. 1987. How do protons cross the membrane-solution interface? Kinetic studies on bilayer membranes exposed to protonophore S-13 (5-chloro-3-tert-2'-chloro-4' nitrosalicylanilide) *J. Membr. Biol.* 95:73–89.
- Kimura, J., S. Miyamae, and A. Noma. 1987. Identification of sodium-calcium exchange currents in single ventricular cells of guinea-pig. *J. Physiol.* 384:199–222.
- Mogul, D. J., D. H. Singer, and R. E. Ten Eick. 1989. Ionic diffusion in voltage-clamped isolated cardiac myocytes. *Biophys. J.* 56:565–577.
- Nakao, M., and D. C. Gadsby. 1989. Na and K dependence of the Na/K pump current-voltage relationship in guinea pig ventricular myocytes. *J. Gen. Physiol.* 94:539–565.
- Neher, E. 1986. Concentration profiles of intracellular calcium in the presence of a diffusible chelator. *Exp. Brain Res.* 14:80–96.
- Neher, E. 1988. The influence of intracellular calcium concentration on degranulation of dialysed mast cells from rat peritoneum. *J. Physiol.* 395:193–214.
- Noble, D. 1986. Sodium-calcium exchange and its role in generating electric current. In *Cardiac Muscle: Excitation and Regulation of Contraction*. R. Nathans, editor. Academic Press, NY. 171–199.
- Oliva, C., I. S. Cohen, and R. T. Mathias. 1988. Calculation of time constants for intracellular diffusion in whole cell patch clamp configuration. *Biophys. J.* 54:791–799.
- Press, W. H., B. P. Flannery, S. A. Teukolsky, and W. T. Vetterling. 1986. *Numerical Recipes*. Cambridge Univ. Press, New York.
- Pusch, M., and E. Neher. 1988. Rates of diffusional exchange between small cells and a measuring patch pipette. *Pfluegers Arch. Eur. J. Physiol.* 411:204–211.